Supporting Information on

Novel magnetite nanorods decorated Si-Schiff base complex for efficient immobilization of U(VI) and Pb(II) from water solutions

Ayub Khan, Jinlu Xing, Ahmed Mourtada Elseman, Pengcheng Gu, Kashif Gul, Yuejie Ai,* Riffat Jehan, Ahmed Alsaedi, Tasawar Hayat and Xiangke Wang*

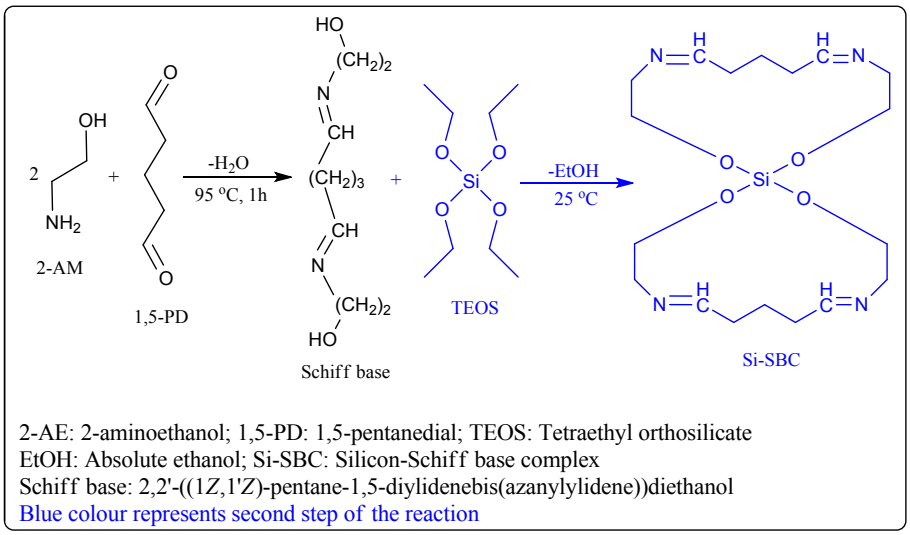

Scheme S1 Schematic representation of the synthesis of Schiff base and its silicon complex.

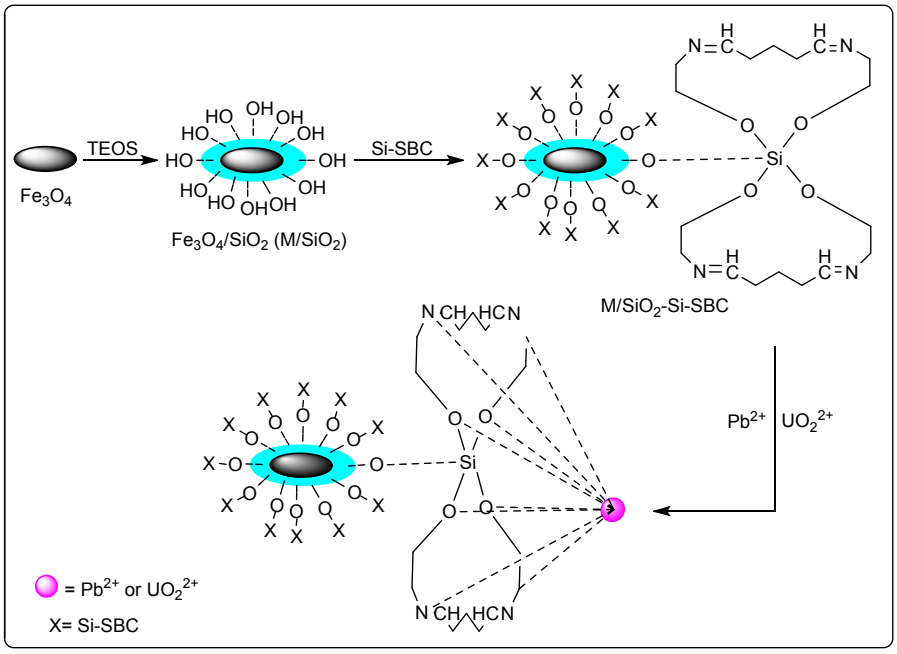

Scheme S2 Synthesis of M/SiO_2-Si-SBC and its interaction with metal ions.

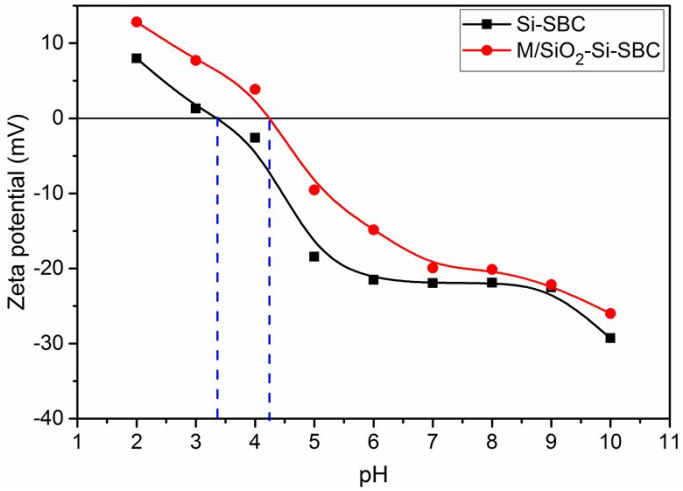

Fig. S1 Point of zero charge of Si-SBC and M/SiO_2-Si-SBC.

NMR study of Schiff base

The ^{1}H NMR spectral data (Fig. S2) of SB are recorded in DMSO-d_6 for the evaluation of the number and nature of all the protons relative to TMS with chemical shifts given in ppm (DMSO-d_6=0 ppm). All the protons resonated at appropriate positions, i.e., CH_2-OH hydrogen appeared as a triplet at δ=3.38-3.36 ppm. Similarly, the aliphatic protons attached to C-8 and C-11 had the same chemical environment and gave triplet at δ=1.09-1.06 ppm, the azomethine hydrogens (CH=N) gave singlet at δ=3.42 ppm, the aliphatic hydrogens attached to C-2 and C-4, appeared as triplet at δ=2.58-2.56 ppm, and finally the two protons attached to C-3 gave quartet at δ=3.48-3.44 ppm. The proton-decoupled ^{13}C NMR spectrum (Fig. S3) revealed that SB had five different carbon atoms. C-2 and C-4, highly shielded, appeared up-field at δ=18.58 ppm, C-3 appeared at δ=39.98-38.97 ppm, C-8 and C-11 appeared at δ=44.17 ppm, CH=N was deshielded and appeared at δ=56.56 ppm, the C-7 and C-12 were also highly deshielded due to –OH group and appeared down-field at δ=63.48 ppm.

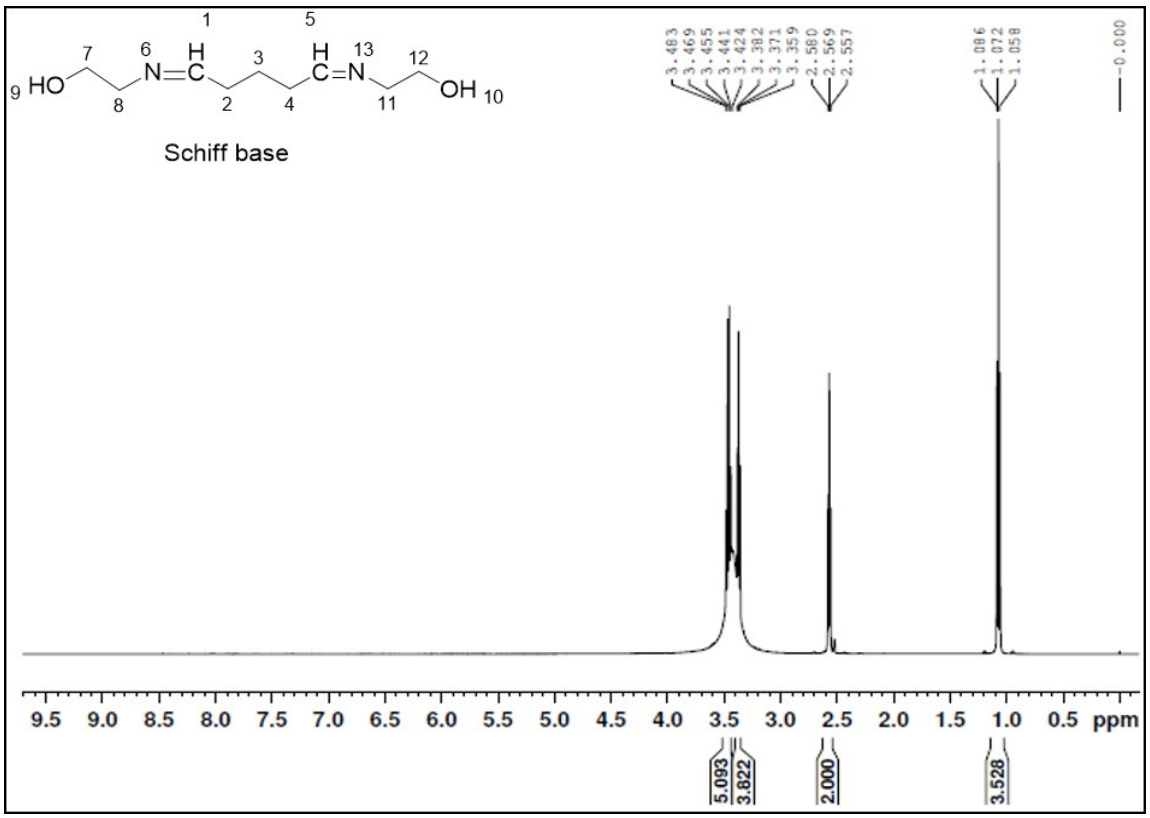

Fig. S2 ^{1}H NMR spectrum of Schiff base.

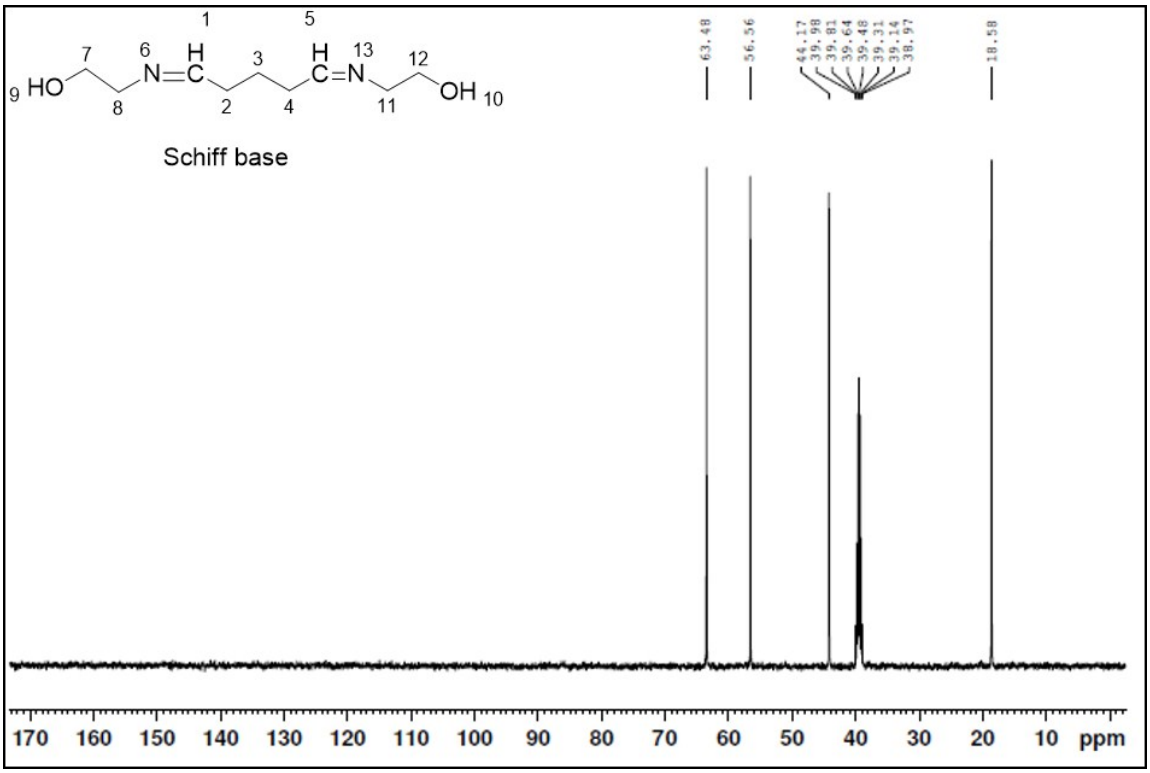

Fig. S3 ^{13}C NMR spectrum of Schiff base.

Effect of pH on the adsorption of U(VI)

The relative speciation of U(VI) species (Fig. 4D) showed that at pH 7.0, UO_2^{2+}, $(UO_2)_2(OH)_2^{2+}$, UO_2OH^+, $(UO_2)_3(OH)_5^+$, and $(UO_2)_4(OH)_7^+$ ions were the dominant species in solution. At lower pH values, there was competition between H^+, Na^+, and UO_2^{2+} ions for sorption sites, which suppressed the sorption of UO_2^{2+} ions.[1] The high adsorption efficiency at pH 7.0-9.0 was due to the strong surface complexation and electrostatic interactions between the positively charged U(VI) species and the negatively charged Si-SBC and M/SiO_2-Si-SBC surfaces. At pH > 9.0, the electrostatic repulsion between U(VI) anions such as $(UO_2)_3(OH)_7^-$, $UO_2(OH)_3^-$, and $(UO_2)(OH)_4^{2-}$ and the negatively charged surfaces of Si-SBC and M/SiO_2-Si-SBC resulted in low adsorption.[2]

Table S1 Kinetic parameters of Pb(II) and U(VI) sorption on Si-SBC and M/SiO_2-Si-SBC at 25 °C

Model	Parameters	Pb(II)		U(VI)	
		Si-SBC	M/SiO_2-Si-SBC	Si-SBC	M/SiO_2-Si-SBC
Pseudo-first-order	k_1 (1/h)	0.5968	1.002	1.0161	1.0335
	$q_{e,cal}$ (mol/g)	3.43×10^{-4}	4.23×10^{-4}	2.03×10^{-4}	2.94×10^{-4}
	R^2	0.9881	0.9837	0.9449	0.9573
Pseudo-second-order	k_2 (g/mol·h)	2029.04	3380.06	5947.11	4514.51
	$q_{e,cal}$ (mol/g)	3.78×10^{-4}	4.52×10^{-4}	2.20×10^{-4}	3.16×10^{-4}
	h (mol/g·h)	2.90×10^{-4}	6.89×10^{-4}	2.88×10^{-4}	4.51×10^{-4}
	$t_{1/2}$ (h)	1.3041	0.6551	0.7641	0.7008
	R^2	0.9913	0.9989	0.9848	0.9903
Intraparticle diffusion Stage-I	k_{p1} (mol/g·$h^{1/2}$)	2.15×10^{-4}	2.00×10^{-4}	1.58×10^{-4}	1.78×10^{-4}
	C_1 (mol/g)	-6.00×10^{-5}	6.35×10^{-5}	-2.30×10^{-5}	5.57×10^{-6}
	R_1^2	0.9823	0.9505	0.8837	0.8556
Stage-II	k_{p2} (mol/g·$h^{1/2}$)	5.80×10^{-5}	6.21×10^{-5}	3.23×10^{-5}	5.26×10^{-5}
	C_2 (mol/g)	1.73×10^{-4}	2.60×10^{-4}	1.06×10^{-4}	1.45×10^{-4}
	R_2^2	0.9832	0.9545	0.9857	0.8859
Stage-III	k_{p3} (mol/g·$h^{1/2}$)	1.16×10^{-5}	6.32×10^{-6}	6.60×10^{-6}	4.08×10^{-6}
	C_3 (mol/g)	2.94×10^{-4}	4.04×10^{-4}	1.84×10^{-4}	2.87×10^{-4}
	R_3^2	0.9625	0.9603	0.9734	0.9585

Separation factor (RL)

The dimensionless constant separation factor (R_L), given in Eq. (S1), expresses the most important characteristics of the Langmuir isotherm:[3]

$$R_L = \frac{1}{1 + bC_o} \qquad (S1)$$

The value of R_L describes the nature of equilibrium and falls to zero (R_L=0) for the irreversible process. The equilibrium is more favourable when 0 < R_L < 1 and linear when R_L=1, whereas the equilibrium is unfavourable when R_L > 1.[4] For the adsorption of U(VI) and Pb(II) onto Si-SBC and M/SiO_2-Si-SBC, the obtained R_L values were plotted against the initial concentrations of U(VI) and Pb(II) and are shown in Fig. S4. It indicated that the R_L values were dependent on temperature

and concentration of U(VI) and Pb(II). One can see from Fig. S4 that the values of R_L are between 0.0176 and 0.2925 for Pb(II) and 0.0075 and 0.3126 for U(VI) on Si-SBC and M/SiO_2-Si-SBC respectively. Moreover, it is clear from the Fig. S4 that at all temperatures, the adsorption of U(VI) and Pb(II) was more favorable at low concentrations and became nearly irreversible at high initial concentrations of the metal ions.

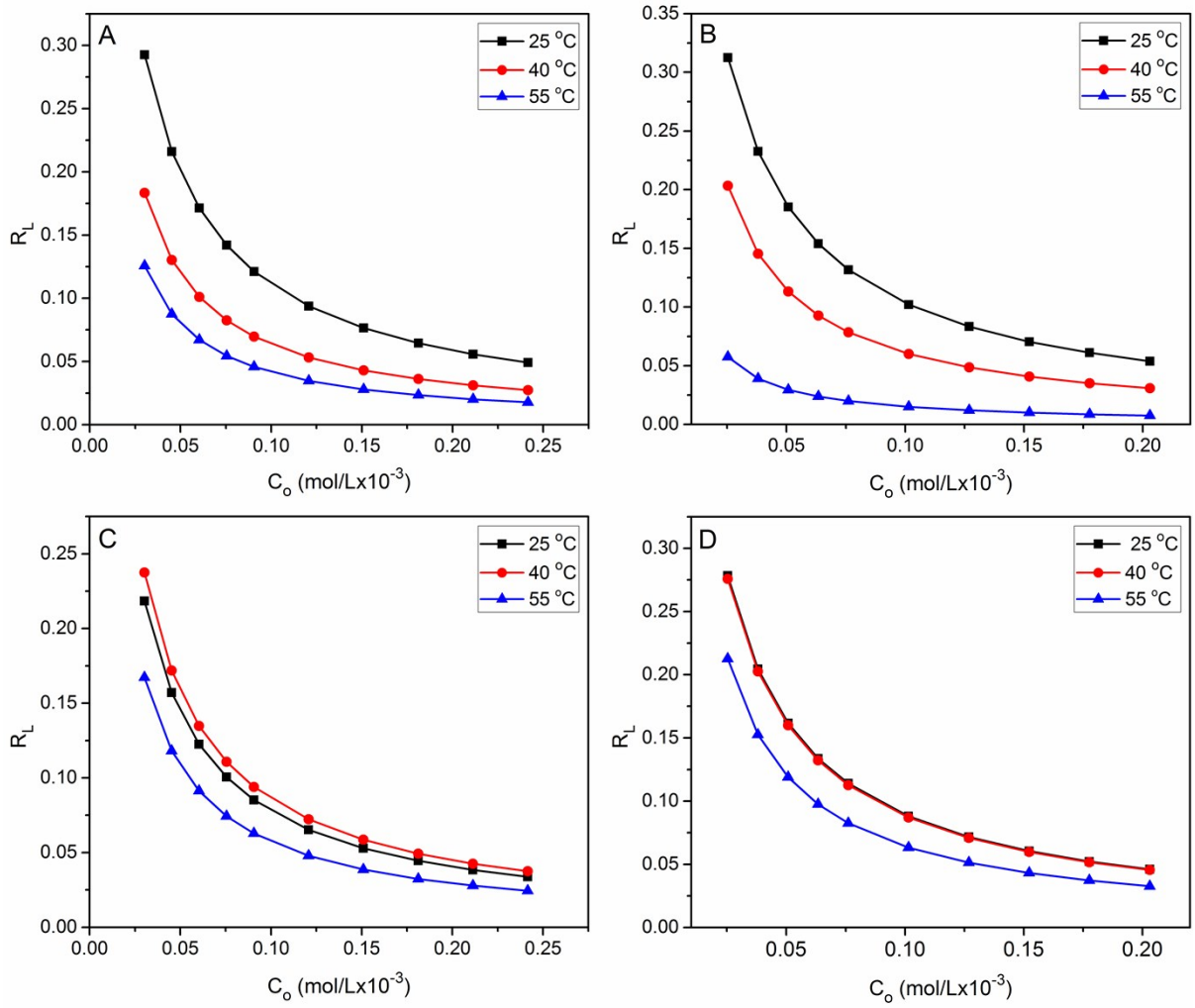

Fig. S4 Separation factors for the adsorption of: Pb(II) (A) and U(VI) ions (B) onto Si-SBC and Pb(II) (C) and U(VI) ions (D) onto M/SiO_2-Si-SBC.

Table S2 The parameters for Freundlich and Sips isotherms of Pb(II) and U(VI) sorption on Si-SBC and M/SiO_2-Si-SBC at different temperatures

Isotherm model	Parameters	Pb(II)					
		Si-SBC			M/SiO_2-Si-SBC		
		25 °C	40 °C	55 °C	25 °C	40 °C	55 °C
Freundlich	n	0.2859	0.2516	0.2746	0.2673	0.3158	0.3475
	K_F ($mol^{1-n}\cdot L^n/g$)	6.38×10^{-3}	6.23×10^{-3}	1.07×10^{-2}	7.22×10^{-3}	1.60×10^{-2}	3.11×10^{-2}
	R^2	0.9588	0.9554	0.9754	0.9663	0.9421	0.912
Sips	q_m (mol/g)	5.65×10^{-4}	7.30×10^{-4}	9.80×10^{-4}	6.96×10^{-4}	8.60×10^{-4}	9.88×10^{-4}
	K_s (L/g)	6.47×10^{4}	9.74×10^{4}	9.65×10^{4}	9.72×10^{4}	1.08×10^{5}	1.78×10^{5}
	n	0.7989	0.6574	0.5808	0.8188	1.0140	1.0740
	R^2	0.9937	0.9839	0.9919	0.9968	0.9942	0.9846
		U(VI)					
Freundlich	n	0.3021	0.2649	0.1868	0.3073	0.3276	0.3147
	K_F ($mol^{1-n}\cdot L^n/g$)	5.54×10^{-3}	5.26×10^{-3}	3.09×10^{-3}	7.93×10^{-3}	1.31×10^{-2}	1.41×10^{-2}
	R^2	0.9691	0.9879	0.9645	0.9555	0.9706	0.944
Sips	q_m (mol/g)	4.29×10^{-4}	6.91×10^{-4}	1.15×10^{-3}	5.02×10^{-4}	7.38×10^{-4}	7.02×10^{-4}
	K_s (L/g)	5.76×10^{4}	3.44×10^{4}	6.03×10^{3}	9.21×10^{4}	6.78×10^{4}	1.52×10^{5}
	n	0.7411	0.4838	0.2693	0.9056	0.7612	1.0417
	R^2	0.9944	0.9987	0.9628	0.9971	0.9954	0.9905

Effect of temperature and metal ion concentration

Fig. S5 gives the effect of temperature and metal ion concentration on the adsorption of U(VI) and Pb(II) ions. Fig. S5A-5D show that the adsorption percentages of U(VI) and Pb(II) increase with the increase of temperature from 25 to 55 °C. This is because, the kinetic energy of the metal ions increases with the increase of temperature and their approach to the adsorbent surface becomes easier. However, a rapid decrease is found in the percentage adsorption of U(VI) and Pb(II) ions with the increase in their initial concentrations from 3.02×10^{-5}-2.42×10^{-4} mol/L and 2.54×10^{-5}-2.03×10^{-4} mol/L respectively. On the other hand, the amounts of U(VI) and Pb(II) adsorption increase rapidly with the increase of temperature and initial concentration of metal ions (Fig. S5E-5H). This is because, the high initial concentration provided a significant driving force to overcome all the mass transfer resistances between the metal ions and the solid particles.[5]

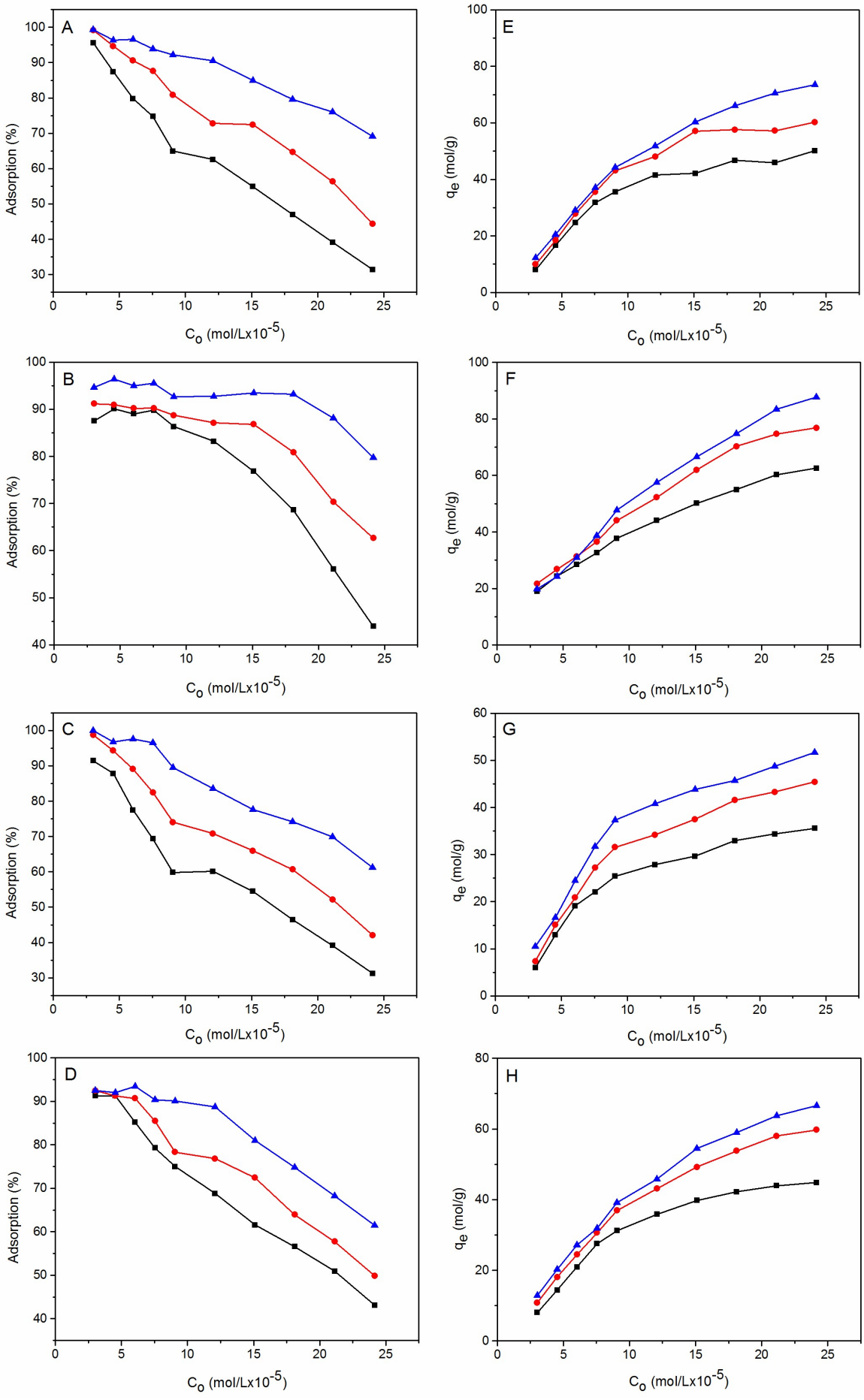
A
Adsorption (%)
C_o (mol/Lx10^{-5})
E
q_e (mol/g)
C_o (mol/Lx10^{-5})
B
Adsorption (%)
C_o (mol/Lx10^{-5})
F
q_e (mol/g)
C_o (mol/Lx10^{-5})
C
Adsorption (%)
C_o (mol/Lx10^{-5})
G
q_e (mol/g)
C_o (mol/Lx10^{-5})
D
Adsorption (%)
C_o (mol/Lx10^{-5})
H
q_e (mol/g)
C_o (mol/Lx10^{-5})

Fig. S5 The effect of temperature and initial concentrations on the percentage adsorption of Pb(II) (A, B), and U(VI) (C, D) on Si-SBC and M/SiO_2-Si-SBC, respectively. The effect of temperature and initial concentrations on amount of adsorption of Pb(II) (E, F), and U(VI) ions (G, H) on Si-SBC and M/SiO_2-Si-SBC, respectively at pH=5.00±0.05, C[$NaNO_3$]=0.01 mol/L, solid content=0.150 g/L, and contact time=24 h; -■-=25 °C, -●-=40 °C, and -▲-=55 °C.

References

1 X. Wang, Q. Fan, S. Yu, Z. Chen, Y. Ai, Y. Sun, A. Hobiny, A. Alsaedi and X. Wang, *Chem. Eng. J.*, 2016, **287**, 448-455.

2 C. Ding, W. Cheng, Y. Sun and X. Wang, *Geochim. Cosmochim. Acta*, 2015, **165**, 86-107.

3 T. Weber and R. Chakravorti, *AlChE Journal*, 1974, **20**, 228-238.

4 K. R. Hall, L. C. Eagleton, A. Acrivos and T. Vermeulen, *I&EC Fundam*, 1966, **5**, 212-223.

5 B. H. Hameed, *J. Hazard. Mater.*, 2009, **161**, 753-759.